Published in final edited form as:
*Neuroreport*. 2002 December 20; 13(18): 2487–2492. doi:10.1097/01.wnr.0000047685.08940.d0.

# Simultaneous EEG and fMRI of the alpha rhythm

**Robin I. Goldman**[2,CA], **John M. Stern**[1], **Jerome Engel Jr**[1], and **Mark S. Cohen**
Ahmanson-Lovelace Brain Mapping Center, UCLA, 660 Charles Young Drive South, Los Angeles, CA 90095

[1]Department of Neurology, UCLA School of Medicine, Los Angeles, CA

[2]Hatch Center for MR Research, Columbia University, HSD, 710 W.168th St., NIB-1, Mailbox 48, NY, NY10032, USA

## Abstract

The alpha rhythm in the EEG is 8–12 Hz activity present when a subject is awake with eyes closed. In this study, we used simultaneous EEG and fMRI to make maps of regions whose MRI signal changed reliably with modulation in posterior alpha activity. We scanned 11 subjects as they rested with eyes closed. We found that increased alpha power was correlated with decreased MRI signal in multiple regions of occipital, superior temporal, inferior frontal, and cingulate cortex, and with increased signal in the thalamus and insula. These results are consistent with animal experiments and point to the alpha rhythm as an index of cortical inactivity that may be generated in part by the thalamus. These results also may have important implications for interpretation of resting baseline in fMRI studies.

### Keywords

Alpha rhythm; BOLD; EEG; fMRI; Resting state; Simultaneous; SITE

## INTRODUCTION

In Berger's first EEG recordings from the human scalp in the late 1920s, he noticed a prominent sinusoidal wave of around 10 cycles/s that he later named the alpha rhythm [1]. The EEG of most adults contains this 8–12 Hz signal in occipital, parietal and posterior temporal regions [2]. The alpha rhythm (alternatively called the posterior dominant rhythm) is highest in amplitude when a subject is awake and relaxed with eyes closed, and is attenuated by opening the eyes and by mental effort, as well as by drowsiness or sleep [3].

Although recognized since the beginnings of EEG, the functional significance of the alpha rhythm in humans is not known definitively. Alpha band activity has been used as an indirect measure of brain activation because increased activity in this frequency range is thought to correspond to decreased functional activity in underlying cortex [4]. Because the alpha rhythm is present only when a subject is awake, the loss of this rhythm is used clinically to signify the first stages of sleep [5]. Alpha activity also has been studied in event-related paradigms that have pointed to alpha as a marker of visual attention [6] generated in part by retinotopic visual areas [7].



[CA]Corresponding Author and Address: rg2146@columbia.edu.

Studies in both animals and humans have shown the thalamus and regions of occipital and parieto-occipital cortex to be involved in alpha rhythm generation. Using electrodes implanted in dogs, Lopes da Silva demonstrated significant thalamo-cortical coherences in the lateral geniculate nucleus and pulvinar [8,9] and also found alpha sources in dog visual cortex [10]. Studies of spontaneous alpha in humans using MEG have shown sources of the posterior alpha rhythm around both the parieto-occipital and calcarine sulci [11]. The identification of generator regions using scalp EEG or MEG alone, however, is challenged by the fundamental difficulties in localizing sources in a conductive volume from only surface information (the 'inverse' problem [12]).

At least three groups of investigators have used EEG in concert with medical imaging techniques in an attempt to localize the alpha rhythm in humans. Sadato and colleagues looked at changes in alpha power using $O^{15}$-water PET [13]; they recorded EEG simultaneously with PET in normal volunteers while the subject's eyes were open. They then produced statistical maps of the correlation between alpha power in the posterior electrodes and blood flow from the PET images. Sadato's group reported that relative cerebral blood flow (rCBF) increased in the right thalamic region, areas of the pons and midbrain and parts of the limbic system including the hypothalamus, right amygdala, basal frontal cortex and insula as alpha power increased (positive correlation). They found also that increases in alpha power were associated with decreased rCBF (negative correlation) in the bilateral occipital cortex, including primary and association visual areas, as well as the left dorsomedial prefrontal cortex.

Larson [14] and Lindgren [15] examined the relationship between alpha power and the thalamic metabolic rate of glucose using fluoro-deoxyglucose PET and EEG acquired just prior to PET scanning in normal controls and in depressed subjects. Unlike Sadato, both Larson and Lindgren found that global alpha power was correlated inversely with the thalamic rate of glucose metabolism. Larson found this across subjects, whereas Lindgren found no thalamic correlation in subjects who were depressed.

By interleaving EEG and functional MRI recording, Singh and colleagues used an eyes open *vs* eyes closed paradigm [16] and a relaxation *vs* mental arithmetic paradigm with eyes closed [17] to observe the blood oxygenation level dependent (BOLD) response in the parietal and occipital lobes correlated with occipital alpha rhythm. The EEG was recorded in blocks between functional scans. In each study, they found a negative BOLD response (indicative of decreased blood flow [18,19]) in portions of the occipital lobe correlated with increased power in the alpha band.

In the present experiment, we used EEG and fMRI acquired simultaneously, which we have termed simultaneous imaging for tomographic electrophysiology (SITE), to localize potential generator regions of the alpha rhythm during eyes closed rest [20]. Unlike the above studies, SITE enables imaging with both high temporal and high spatial resolution.

## MATERIALS AND METHODS

### Subjects

Eleven normal volunteers (mean age 30, range 23–43, five females) participated in the study. The subjects were in various states of drowsiness at the time of scanning (see Discussion). All subjects gave informed consent approved by the UCLA Human Subject Protection Committee.

## Study design

We recorded simultaneous EEG and fMRI on all subjects while they were at rest with their eyes closed. No visual or auditory stimuli were presented at any time during functional scanning beyond the ambient scanner noise, which was continuous regardless of alpha levels. Each subject underwent either two consecutive 4 min 30 s or three consecutive 9 min functional scans. Two of the 11 subjects were scanned on multiple days (subject A, 3 days; subject B, 2 days).

## EEG

EEG was recorded from 16 scalp sites of the international 10–20 system in a hard-wired bipolar montage (Fp2-F8, F8-T4, T4-T6, T6-O2, O2-P4, P4-C4, C4-F4, F4-Fp2; Fp1-F7, F7-T3, T3-T5, T5-O1, O1-P3, P3-C3, C3-F3, F3-Fp1) using silver/silver chloride coated plastic cup electrodes, each of which was equipped with dual carbon fiber leads. This allowed each lead pair to be twisted together to reduce artifacts caused by induced EMF in the MR scanner. The EEG system was designed specially for in-magnet recording by our lab in collaboration with Grass-Telefactor (a division of Astro-Med, Inc., West Warwick, RI) and has been described in detail elsewhere [21]. With this system, artifact in the EEG due to gradients and radio frequency noise appears only while each slice is being collected. By spacing slice acquisition evenly through the TR period, windows of EEG are visible between gradient bursts. By reducing the MR brain coverage to six slice planes, we were able to record interpretable EEG during 87% of each TR period [21]. We have since developed a method for recording simultaneous EEG/fMRI without this restriction [22,23].

## Scanning

We performed all scans on a General Electric 3 T imager with Echo Planar Imaging (EPI) capability provided by Advanced NMR Systems. We acquired a sagittal localizer scan to set up the orientation of the functional slice planes. We then collected functional EPI gradient-echo scans (TR = 2500 ms, TE = 45 ms, 80° flip angle, 20 × 20 cm FOV, 64 × 64 matrix, 4 mm skip 1 mm) in six adjacent slice planes, with the second most inferior slice oriented through the anterior commissure-posterior commissure (AC-PC) line to ensure consistency of slice planes across subjects. The slice locations were chosen to include the thalamus and a majority of the occipital lobe. We also acquired a co-planar high-resolution spin echo EPI scan (TR = 4000 ms, TE = 54 ms, 20 × 20 cm FOV, 128 × 128 matrix) to serve as an anatomic reference for the functional scans.

## Data analysis

Whether acquired as 9 min or 4 min 30 s studies, functional scans were broken into 4 min 30 s segments to compare across subjects. Using FSL software (http://www.fmrib.ox.ac.uk/fsl), functional images were motion corrected, spatially smoothed (FWHM = 5 mm) and highpass filtered (cut-off 150 s) to attenuate low frequency drift. EEG was post-processed using software developed in-house [21] to remove scanner artifacts and ballistocardiographic artifact, which is present due to the small pulse-related translations of the scalp in the static magnetic field.

In order to focus specifically on the posterior dominant rhythm (and not other rhythms in the alpha range such as the mu rhythm over the motor cortex), only the four bipolar channels containing occipital electrodes (T6-O2, O2-P4, T5-O1, O1-P3) were included in further analyses. Using a Fast Fourier Transform, we calculated the power in the alpha band in 2.5 s epochs corresponding to each TR for each of these four bipolar channels. The average of the alpha power at each epoch across the four channels, $P_{\alpha}(t)$, was then calculated and used for image analysis. Periods of EEG that, by visual inspection, appeared to contain minor motion

or muscle artifact were discarded and replaced by interpolating the alpha band power linearly between segments before and after the artifact. We then convolved the resulting alpha power curves with an *a priori* hemodynamic response function [24] and performed a voxel-wise correlation to yield fMRI maps using scanSTAT (Cohen MS. *Methods* **25**, 201–220 (2001)). The statistical maps were superimposed onto the high-resolution EPI images of each subject acquired in the same scan session (Fig. 1).

The sensitivity of the BOLD method depends upon the modulation of an independent variable; we used the following unbiased method for selecting sessions with substantial alpha fluctuation to be included in the analysis. To compare depth of alpha modulation across scans, we used the coefficient of variation (CV), calculated for each scan as $CV_\alpha = \sigma_{P(t)}/P(t)$, where $\sigma_{P(t)}$ is the standard deviation and P(t) is the average of $P_\alpha(t)$. Because the distribution of $CV_\alpha$ across scans was skewed and unimodal based on a Kolmogorov–Smirnov test, we included in further analyses only the scans with $CV_\alpha$ above the median value of 0.16.

We then quantified motion in the fMRI data using the translational motion estimates from FSL (a six-parameter rigid body model). Motion displacements (max − min) in x, y, and z were added as a vector sum for each scan, and images containing motion greater than one standard deviation from the mean across scans were excluded from further analysis. In addition, correlation maps with strong signal correlation in non-brain areas (such as the ventricles) were discarded.

Due to the reduced slice coverage in this study, the remaining images were compared using regions of interest (ROIs), drawn based on anatomical landmarks in each individual scan. Nine separate ROIs were used, including the thalamus, anterior cingulate, left and right insula, a left and a right region containing the lateral superior temporal and inferior frontal cortex, and three regions in occipital cortex, (1) the occipital pole with adjacent medial occipital cortex, (2) the anterior medial occipital cortex, and (3) the left and right lateral occipital cortex. At a per-voxel correlation threshold of $r \geq 0.3$ (uncorrected $p < 0.001$), we estimated the cluster size for each ROI above which the probability of type I errors was <0.05 using the Monte Carlo simulation AlphaSim [25] with a mask of the dimensions of the ROI and assuming a spatial correlation of FWHM = 8 mm. Only cluster sizes larger than this were included in the ROI analysis. BOLD signal percentage change values for each ROI were calculated as the average slope of the regression line for voxels above the threshold $r \geq 0.3$.

The average and variance of the number of voxels and percentage signal change in each ROI were calculated per subject. If a subject had only one scan, the variance for that subject was calculated using mean imputation of the variance for the remaining subjects. Group statistics were then were calculated across subjects by weighting the within-subject values by the number of scans for that subject. To describe the results more fully, and not obscure zero values, only non-zero ROIs were included in the group calculations and the fraction of non-zero scans per ROI are given (thus, the average for each ROI across all 10 scans can be calculated from Table 1 as [no. voxels] × [fraction nonzero]). Group statistics are presented as the mean ± s.d.

## RESULTS

A total of 34 scan blocks of 4 min 30 s were analyzed, and 15 of these (five subjects) had a $CV_\alpha$ greater than the median value of 0.16. Of these, five scans were discarded due to image motion artifact. The remaining scans (subject A, four scans; subject B, two scans; subject C, three scans; subject D, one scan) are presented here.

Alpha power correlated negatively with MRI signal in the three occipital ROIs. Negative correlations were found also in left and right superior temporal/inferior frontal regions, and in the anterior cingulate region. Positive correlations of alpha power with MRI signal were seen in the thalamus and insula. A representative single subject map is shown in Fig. 2, and the BOLD signal changes for each ROI in this scan are shown in Fig. 3. Because of the high correlation between time courses, the curves for R and L insula ($r = 0.86$), R and L superior temporal/inferior frontal ($r = 0.94$), and the three occipital ROIs ($r \geq 0.91$) have been averaged in Figure 3.

The ROI results for all 10 scans are summarized in Table 1. With the exception of the left insula, all of the ROIs contained voxels with correlation above $r = 0.3$ in at least one scan per subject. The ROI in the left insula, however, contained voxels with correlation above threshold in only two of the four subjects.

## DISCUSSION

We have shown with this study that fMRI can identify brain regions associated with changes in the alpha rhythm. Signal detected by the scalp EEG most likely comes from cortical areas near the recording electrode; however, the fMRI maps of alpha activity presented here include correlated BOLD signal in areas other than the posterior cortex, even though EEG from only posterior electrodes was used. What, then, is the possible role of these correlated regions? We propose that there are three types of regions highlighted by SITE mapping: (1) generator regions of the EEG rhythms themselves, (2) regions that are part of a generating circuit but that do not themselves directly generate the rhythms detected by scalp EEG (e.g. regions at depth such as the thalamus), and (3) regions where activity is correlated with the EEG but not causally linked to rhythm generation (for example, drowsiness corresponded to the alpha power in our experiment but it may have anatomic bases that are independent to the generators of the alpha rhythm). Clearly, the present experiment cannot distinguish among these three.

Our findings are consistent with the notion that the alpha rhythm is an index of reduced cortical activity, and that the thalamus is likely to play a role in producing this active stand-by state. The three occipital regions that showed negative correlation with the alpha rhythm in our experiment (indicating there was less activity in occipital cortex as indexed by BOLD when alpha power was high) also have been identified by others as separate alpha generator regions by independent component analysis (ICA) [26].

Our finding that BOLD response in the insula correlates positively with alpha power replicates Sadato's findings in PET [13] as well as a study by Valdez-Sosa using EEG source modeling (personal communication). Indeed, this result may indicate a physiologic association between insular activity and the alpha rhythm instead of a direct role of the insula in alpha generation. Drowsiness did play a role in alpha modulation in our study in some subjects and thus might be a factor; however, Sadato's experiment was performed in individuals with eyes open, suggesting that the correlation in the insula was not due solely to drowsiness.

We, as well as Sadato, showed a positive correlation with alpha power in the thalamus. However, both Larson and Lindgren found a negative correlation between alpha power and thalamic glucose metabolism. While at first these studies seem contradictory, they actually may highlight different thalamic contributions. Because of the low temporal resolution of FDG-PET (30 min), Larson and Lindgren were not able to look at phasic changes in the EEG on an individual subject level. Therefore, their experimental results may point to trait-like properties of alpha generation across subjects. Our findings with fMRI, as well as those

of Sadato (collected in 90 s time points), instead reflect alpha modulation on an individual subject level, and thus may highlight the role of the thalamus in moment-to-moment wave generation.

Alpha power fluctuates relatively rapidly, so that delayed imaging [14,15] or interleaved studies [13] run the risk of decreased sensitivity or accuracy from misidentified periods of increase or decrease in alpha power. Thus, the development of tools for simultaneous collection of EEG and fMRI data is particularly significant. Compared to interleaved methods, it is also notable that the scanner noise in our studies was continuous and therefore unlikely to act as a modulator of alpha energy.

This study may also have important implications for interpretation of resting state brain activity. fMRI is a method of mapping changes in brain hemodynamics, and many studies utilize a resting state as a contrast to the activation task of interest. However, BOLD activity during this resting baseline varies widely. Some groups have investigated the variation present in baseline measures [27–29], and have found high correlation among functionally connected regions. As the present study was conducted entirely while the subjects were at rest with their eyes closed, we have shown that alpha rhythm changes may account for at least some of the BOLD changes seen in baseline measures of alpha correlated brain regions.

Although subjects in our study reported being in various states of drowsiness in post-scan interviews, the relationship between depth of alpha rhythm modulation and drowsiness was not consistent. Nonetheless, the alpha rhythm modulation during at least some of the scans may have been due to fluctuating drowsiness levels. Thus, our fMRI maps may show BOLD correlation with drowsiness as well as with the alpha rhythm. Our results, however, were consistent across subject and scan, and are also consistent with existing theory on sources of the alpha rhythm as well as other imaging studies of non-drowsy subjects. Additional SITE experiments that distinguish between waking alpha rhythm and drowsiness are necessary to decipher which anatomical regions are involved in each.

## CONCLUSION

SITE is a potentially powerful tool for mapping EEG sources. It combines the spatial localizing power of fMRI with the electrophysiological information obtainable from EEGs. Here, using fMRI, we mapped spontaneous changes in cerebral activity as identified by the EEG, and for the first time, used simultaneous EEG and fMRI to map potential generators of the alpha rhythm. Our study is consistent with prior human and animal studies that identify occipital cortex, thalamus, and possibly other cortical regions as alpha sources.

Our approach can be applied, without modification, to the study of other EEG spectral components associated with brain activity that occur at rest, with cognitive tasks, and with changes in global state such as sleep and depression. Furthermore, these general methods are equally applicable to studies of other electrical phenomena, such as interictal epileptiform discharges and event-related potentials.

## Acknowledgments

We thank James Sayre for statistics advice and Susan Bookeimer for her neuroanatomy expertise. This work was supported in part by grant number R01-DA13054-01 from the National Institute on Drug Abuse. R.I.G. was supported by the Epilepsy Foundation and a UCLA Eugene Cota-Robles Fellowship. We receive support from the Brain Mapping Medical Research Foundation, The Ahmanson, Pierson-Lovelace, Jennifer Jones Simon, and Tamkin Foundations, the UCLA Council on Research, and the Grass-Telefactor Division of Astro-Med, Inc.

## References


1. Berger H. J Psychol Neurol. 1930; 40:160–179.
2. Adrian ED, Matthews BHC. Brain. 1934; 57:355–385.
3. Niedermeyer, E. The normal EEG of the waking adult. In: Niedermeyer, E.; Lopes da Silva, F., editors. Electroencephalography: Basic Principles, Clinical Applications, and Related Fields. Baltimore: Williams and Wilkins; 1999. p. 149-173.
4. Shagass, C. Electrical activity of the brain. In: Greenfield, NS.; Sternbach, RA., editors. Handbook of Psychophysiology. New York: Holt, Rinehart and Winston; 1972. p. 263-328.
5. Carskadon, MA.; Dement, WC. Normal human sleep: an overview. In: Kryger, MH.; Roth, T.; Dement, WC., editors. Principles and Practices of Sleep Medicine. Philadelphia: W.B. Saunders Company; 2000. p. 15-25.
6. Foxe JJ, Simpson GV, Ahlfors SP. Neuroreport. 1998; 9:3929–3933. [PubMed: 9875731]
7. Worden MS, Foxe JJ, Wang N, Simpson GV. J Neurosci. 2000; 20:RC63 . [PubMed: 10704517]
8. Lopes da Silva FH, Lierop THv, Schrijer CF, Leeuwen WSv. Electroencephalogr Clin Neurophysiol. 1973; 35:627–639. [PubMed: 4128158]
9. Lopes da Silva FH, Vos JE, Mooibroek J, Van Rotterdam A. Electroencephalogr Clin Neurophysiol. 1980; 50:449–456. [PubMed: 6160987]
10. Lopes da Silva FH, Van Leeuwen WS. Neurosci Lett. 1977; 6:237–241. [PubMed: 19605058]
11. Hari R, Salmelin R, Makela JP, et al. Int J Psychophysiol. 1997; 26:51–62. [PubMed: 9202994]
12. Koles ZJ. Electroencephalogr Clin Neurophysiol. 1998; 106:127–137. [PubMed: 9741773]
13. Sadato N, Nakamura S, Oohashi T, et al. Neuroreport. 1998; 9:893–897. [PubMed: 9579686]
14. Larson CL, Davidson RJ, Abercrombie HC, et al. Psychophysiology. 1998; 35:162–169. [PubMed: 9529942]
15. Lindgren KA, Larson CL, Schaefer SM, et al. Biol Psychiatry. 1999; 45:943–952. [PubMed: 10386175]
16. Patel P, Al-Dayeh L, Singh M. Int Soc Magn Res Med. 1997; 3:1653.
17. Singh M, Patel P, Al-Dayeh L. Int Soc Magn Res Med. 1998; 3:1493.
18. Ogawa S, Tank DW, Menon R, et al. Proc Natl Acad Sci USA. 1992; 89:5951–5955. [PubMed: 1631079]
19. Kwong KK, Belliveau JW, Chesler DA, et al. Proc Natl Acad Sci USA. 1992; 89:5675–5679. [PubMed: 1608978]
20. Goldman, RI.; Stern, JM.; Engel, J.; Cohen, MS. Topographic mapping of alpha rhythm using simultaneous EEG/fMRI. Brighton, UK: Organization for Human Brain Mappin; 2001.
21. Goldman RI, Stern JM, Engel J, Cohen MS. Clin Neurophysiol. 2000; 111:1974–1980. [PubMed: 11068232]
22. Cohen, MS.; Goldman, RI.; Stern, JM.; Engel, J. Simultaneous EEG and fMRI made easy. Brighton, UK: Organization for Human Brain Mapping; 2001.
23. Cohen MS, Goldman RI, Stern JM, et al. 2002 in preparation.
24. Cohen MS. Neuroimage. 1997; 6:93–103. [PubMed: 9299383]
25. Ward, BD. AFNI AlphaSim Documentation. Medical College of Wisconsin; 2000. Simultaneous inference for fMRI data.
26. Makeig S, Westerfield M, Jung TP, et al. Science. 2002; 295:690–694. [PubMed: 11809976]
27. Cordes D, Haughton VM, Arfanakis K, et al. Am J Neuroradiol. 2000; 21:1636–1644. [PubMed: 11039342]
28. Biswal B, Yetkin FZ, Haughton VM, Hyde JS. Magn Reson Med. 1995; 34:537–541. [PubMed: 8524021]
29. Lowe MJ, Mock BJ, Sorenson JA. Neuroimage. 1998; 7:119–132. [PubMed: 9558644]

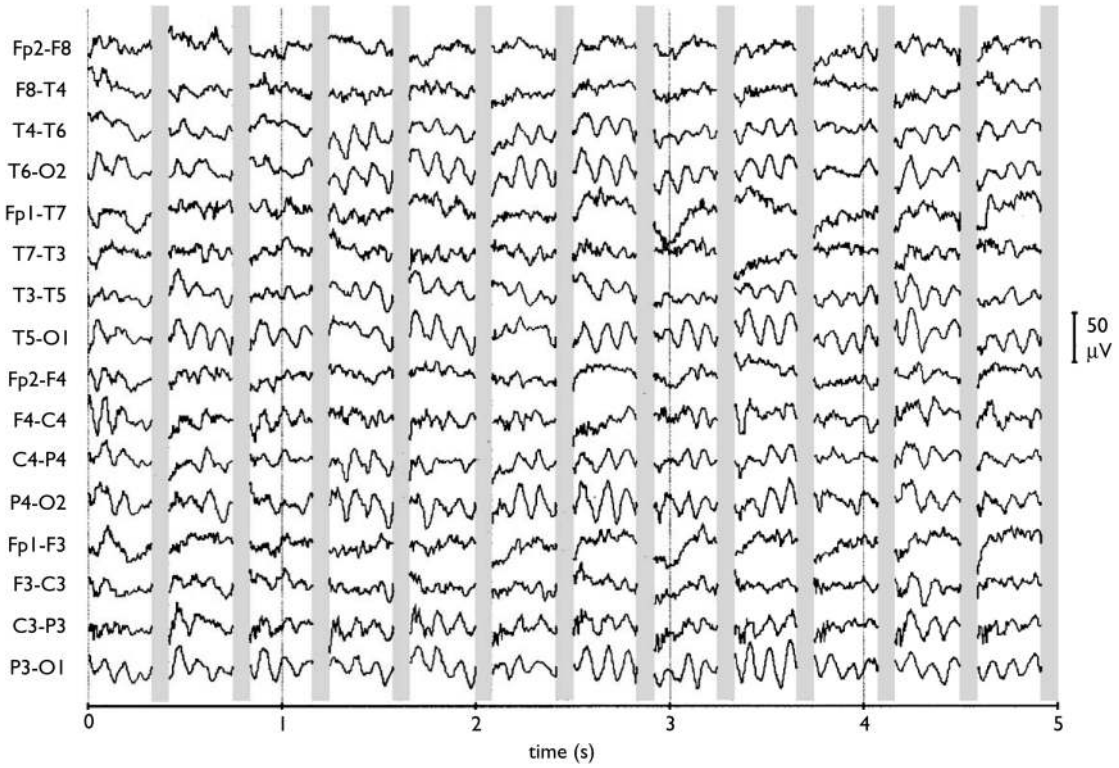


**Fig. 1.**

EEG recorded simultaneously with fMRI. Grey bars indicate 90 ms segments where MR gradient-related artifact was removed. Note clear presence of alpha rhythm in the bipolar channels containing occipital electrodes.

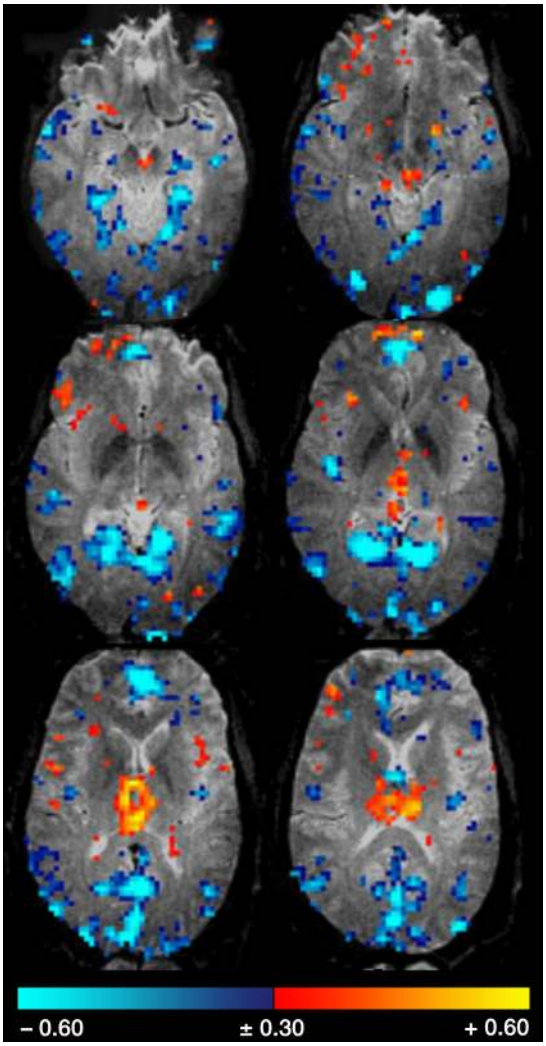


**Fig. 2.**
Regions where MR signal increased (red-yellow) and decreased (blue-cyan) with elevations in alpha power for a representative single subject. The bottom bar shows the Pearson correlation value between signal intensity and alpha power modulation.

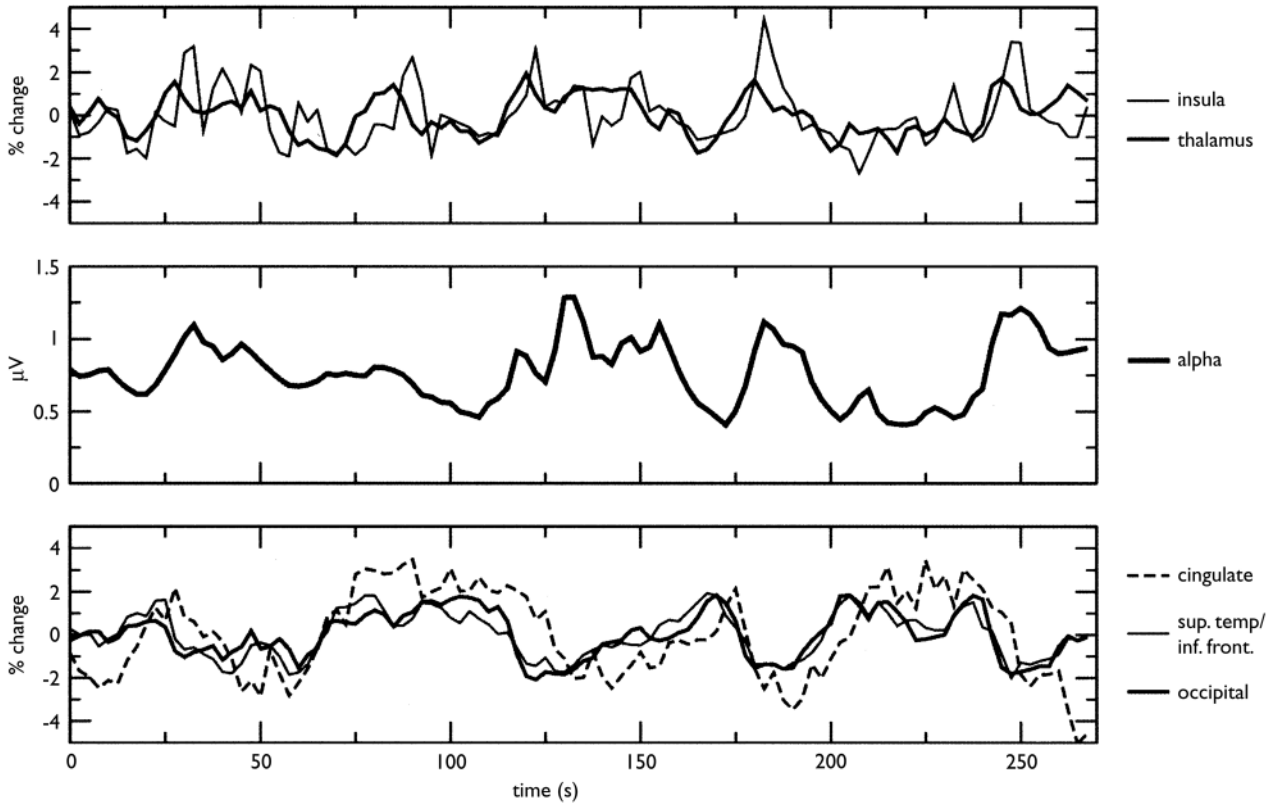


**Fig. 3.**

Time course of the average MRI percentage signal change for ROIs in which BOLD signal was positively (top) and negatively (bottom) correlated with alpha rhythm for the representative single subject shown in Fig. 2. At center is the alpha power time course convolved with a hemodynamic response function, which was used as the independent response model to create the tomographic map of alpha activity.

## Table 1

ROI cluster size (no. voxels) and percentage MR signal change (average slope of the regression line in units of % MR signal change/μV) for voxels with r ≥0.3 in scans where the subject's alpha modulation was greater than the median value of 16% (4 subjects, 10 scans). Only non-zero ROIs are included in the average values, and the fraction of scans with non-zero ROIs are given for each region. Direction of correlation with the alpha rhythm for each ROI is shown.

| Region (direction of correlation) | No. voxels | Percentage signal change | Fraction non-zero |
|---|---|---|---|
| Thalamus (+) | 72 ± 44 | 3.01 ± 0.75 | 0.9 |
| R insula (+) | 11 ± 9 | 3.41 ± 1.20 | 0.8 |
| L insula (+) | 11 ± 5 | 3.22 ± 0.90 | 0.6 |
| Anterior median occipital (−) | 230 ± 121 | 3.42 ± 0.86 | 0.9 |
| Occipital pole (−) | 212 ± 123 | 3.52 ± 0.85 | 0.9 |
| Lateral occipital (−) | 243 ± 188 | 3.38 ± 0.70 | 0.9 |
| Anterior cingulate (−) | 50 ± 15 | 4.08 ± 0.75 | 1.0 |
| R superior temporal/inferior frontal (−) | 99 ± 14 | 2.90 ± 0.58 | 0.7 |
| L superior temporal/inferior frontal (−) | 101 ± 58 | 2.89 ± 0.56 | 0.8 |